Hindawi
Advances in Materials Science and Engineering
Volume 2017, Article ID 5418769, 9 pages
https://doi.org/10.1155/2017/5418769

Research Article

Stochastic Effect of Grain Elongation on Nanocrystalline Materials Strain and Strain Rate Produced by Accumulative Roll-Bonding and Equal Channel Angular Pressing

P. Baonhe Sob,[1] A. Alfayo Alugongo,[1] and T. Ba Bob Tengen[2]

[1]*Department of Mechanical Engineering, Faculty of Engineering and Technology, Vaal University of Technology, Private Bag X021, Vanderbijlpark 1900, South Africa*
[2]*Department of Industrial Engineering and Operations Management, Faculty of Engineering and Technology, Vaal University of Technology, Private Bag X021, Vanderbijlpark 1900, South Africa*

Correspondence should be addressed to P. Baonhe Sob; baonhe_sob@rocketmail.com

Received 20 February 2017; Accepted 3 May 2017; Published 12 June 2017

Academic Editor: Paulo M. S. T. De Castro

Severe plastic deformation techniques are acknowledged to produce elongated grains during fabrication of nanostructured materials. Previous models relating grain size to mechanical properties considered only equivalent radius, thus ignoring other approaches of measuring grain sizes such as semiminor axis, semimajor axis, and major axis radii that determine true grain shape. *In this paper, stochastic models of nanomaterials mechanical properties that include the ignored parameters have been proposed.* The proposed models are tested with data from nanocrystalline aluminum samples. The following facts were experimentally observed and also revealed by the models. Grain elongates to a maximum value and then decreases with further grain refinement due to grain breakages. Materials yield stress increases with elongation to a maximum and then decreases continuously. The varying approaches of measuring grain radius reveal a common trend of Hall-Petch and Reverse Hall-Petch Relationship but with different critical grain sizes. Materials with high curvature grains have more enhanced yield stress. Reducing strain rates leads to materials with more enhanced yield stress, with critical strain rates values beyond which further reductions do not lead to yield stress enhancement. It can be concluded that, by considering different approaches of measuring grain sizes, reasons for different yield stress for nanomaterials that were observed but could not be explained have been dealt with.

1. Introduction

Amongst the severe plastic deformation (SPD) techniques developed and tested, the Equal Channel Angular Pressing (ECAP) and Accumulative Roll-Bonding (ARB) are unique due to their abilities to produce nanomaterials with ultrafine grain structures and high shear strains [1, 2]. The ECAP produces high shear strain without changing the sample shape or dimension [1, 2]. Its main shortcoming is that only small quantities of nanomaterials can be produced during experimentation, which makes it not suitable for industrial application. However, the ARB solves this "small quantity" problem due to its ability to improve on productivity of bulk nanostructure. Both ECAP and ARB are unique and similar since both methods involve large misorientation-angle grain boundaries that lead to very high strains during the deformation of nanostructures [3, 4].

Materials are called nanomaterials because of their refined grain sizes, and most nanomaterials properties have been characterized as a function of their grain sizes or sizes of the constituent structures. The sizes of 3D grain can be described by the equivalent radius r, semiminor axis radius r_2, semimajor axis radius r_1, and major axis radius r_3. Hillert [5] initially established the model for evolution of grain size or grain growth assuming spherical grains while employing the Theory of Second Phase Particle Coarsening. Tengen [6] further states that the theoretical and experimental investigations reveal that grain growth not only is brought about by Grain Boundary Migration (GBM), but also is accompanied by Grain Rotation-Coalescence (GRC)

mechanism. Tengen [6] modified the Hillert Model [5] so as to consider GRC mechanism, the random or stochastic nature of grain size by adding fluctuation terms that account for random fluctuations due to GBM and GRC processes, and variable grain boundary energy.

Despite these modifications of the models for grain size evolutions, most nanomaterials mechanical properties are given as functions of spherical grains [7, 8] although with random size distribution. The relationship between grain size (i.e., equivalent radius) and yield stress was first proposed by Hall and Petch [7, 8]. The Hall-Petch Relationship (HPR) states that as the average size of the grains in materials gets finer, the yield stress increases. This relationship has its shortcoming since infinite refinement does not lead to infinite yield stress. The HPR model was modified by Zhao and Jiang [9] to reveal the Reverse Hall-Petch Relationship (RHPR), which was later modified by Tengen et al. [10] to consider the stochastic nature of grain size.

It should be noted that all the above-mentioned modified models dealt only with the equivalent radius r or made the assumptions that the grains in nanomaterials are spherical in nature. Experimentally, this spherical shape of all the grains in nanomaterials is not the case; in fact, majority of the grains in nanomaterials are not nearly spherical nature. Thus, the models that consider that the grains in nanomaterials are spherical ignore other important parameters such as semiminor axis radius r_2, semimajor axis radius r_1, and the major axis radius r_3, which can be used to closely define elongation and shape. It must be remarked here that a grain undergoing elongation during nanomaterial refinement might not change in equivalent radius (with equivalent radius defined as the radius of an equivalent sphere or circle obtained by the displacement method of volume/area measurement). As such, the impacts of grain elongation on nanomaterials mechanical properties cannot be properly addressed with the use of equivalent radius only. *Therefore a stochastic model of grain elongation for 3D grain undergoing severe plastic deformation that considers the various approaches of measuring grain size is necessary, which has been proposed in the current report*. The impacts of the different approaches of measuring grain sizes and the impacts of grain elongations on nanomaterials are then dealt with in this report. The proposed models are tested with data from grain deformation in nanocrystalline aluminum.

2. Methodology

2.1. Experimental Procedure of Accumulative Roll-Bonding (ARB). The experimental setup for ARB is shown schematically in Figure 1(a). The ARB technology made use of conventional rolling facility. In this report two shafts were placed horizontally so that they were free to rotate by means of a mechanically automated operation. Three gauges (load gauge, temperature gauge, and a time gauge or a stop watch) were used during experimentation. One measured the applied force, which caused the deformation; the second gauge measured the temperature at the time of experiment; and the third gauge measured the time of deformation. All rotating shafts were mounted on the support roll cage with roller bearings to prevent friction during motion. Extra support shafts were mounted to ensure stability of the system during operation. Power was transferred from the power generator to the gearbox by a shaft. Drive was also transferred from the gearbox to the rotating beam by a chain drive. During experimentation a plunger connected to another motor was used to force or feed the AA6082-T6 Aluminum (Al) through the rotating shafts. The purpose of this second motor was to control the feed rate or deformation rate or strain rate. The rotating shafts gripped the AA6082-T6 Aluminum sample and forced the sample through the rollers in the first pass.

The deformed AA6082-T6 Aluminum was cut in two pieces and stacked together. Before stacking, the entire surfaces of the strips were degreased with tetrachlorethylene and wire-brushed (stainless steel brush) to achieve good bonding. The materials were joined together in the corners using aluminum wires and subsequently rolled. The whole sequence of "rolling, cutting, face-brushing, degreasing, and stacking" was repeated again for several "passes" until nanomaterials with required characteristics were obtained.

The samples with the deformed microstructures were examined using Transmission Electron Microscopy (TEM). The microstructure was observed to lengthen along the semimajor axis r_3, semimajor axis r_1, and semiminor axis r_2. The observed nanostructures are presented in Figure 1(b).

2.2. Experimental Procedure of Equal Channel Angular Pressing (ECAP). The experiments were carried out as demonstrated by the routes in Figures 2(a) and 2(b) using samples of AA6082-T6 Aluminum. The ECAP die tunnels were designed to intersect "internally" at angle ϕ ($\phi = 90^{\circ}$) but subtended by the arc or curved "external" surface. During fabrication of nanomaterials, a 50-ton hydraulic press was used to press the aluminum sample through the ECAP die shown in Figures 2(a)–2(c). Since it was very difficult to force the AA6082-T6 Aluminum sample through the ECAP die at the point where the two tunnels meet, the AA6082-T6 Aluminum samples were heat-treated before each ECAP pass to enable the sample to pass through the ECAP die, as recommended by other researchers [1]. It was observed that heating the AA6082-T6 Aluminum sample led to grain growth and subjecting the material through the ECAP die led to grain refinement. The samples with the deformed microstructures were examined using TEM to obtain values of semiminor axis radius, semimajor axis radius, and major axis radius.

2.3. Justifications for Material Used for ARB and ECAP Experimentations. In the current study AA6082-T6 was used for the experimentations. Aluminum material is the most used material in domestic and industrial applications. There are several reasons why aluminum material is widely used in severe plastic deformation process. Some of the reasons are that it is easy to deform aluminum material when compared with other materials. It is also easy to bend aluminum samples to the desired shape during experimentations. Aluminum material is lighter and cheaper when compared to other materials. However, since most severe plastic deformations have been carried out on aluminum material, it is therefore easy

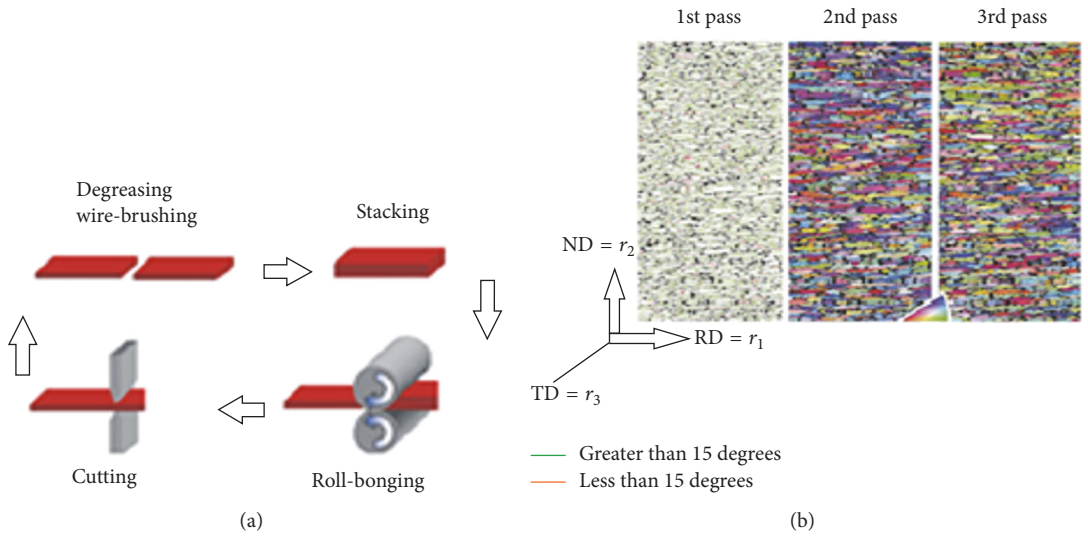

Figure 1: (a) Schematic of ARB experimental setup [11] and (b) microscopic observation.

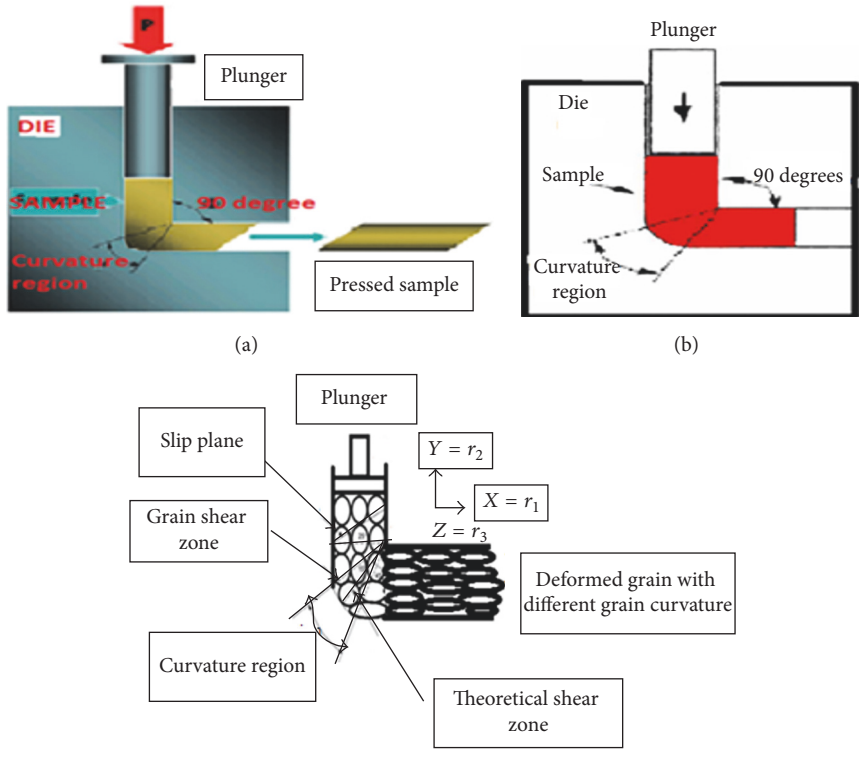

Figure 2: Schematic of ECAP processing routes by Estrin and Vinogradov [1], (a) illustration of material deformation, (b) schematic of material deformation, and (c) schematic of grain refinement.

to compare and validate experimental results and theoretical results, which is critical aspect.

2.4. Sample Preparation for TEM Examination. Standard TEM thin foils that were 3 mm in diameter were prepared by electrolytic twin jet polishing (at −30°C, 30 V) in Struers Tenupol 2 filled with 6% solution of perchloric acid in methanol. The 3D observations were carried out at 200 KV with JEOL JEM 2000FX microscope equipped with an X-ray energy dispersive spectrometer (XEDS) LINKAN 10000.

2.5. Schematic of Experimental Observation Needed for Models Derivations. The material dealt with in this research had grains that were assumed to be initially closely spherical as

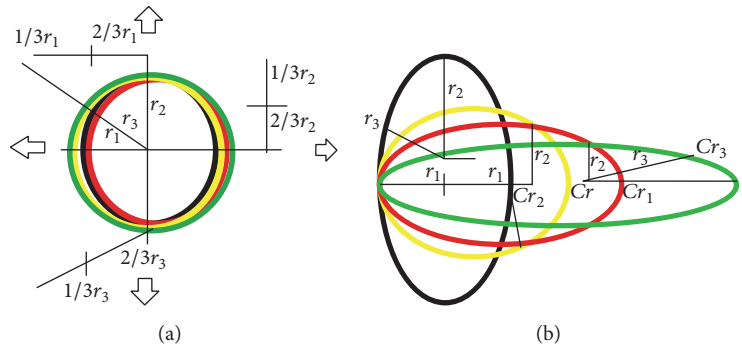

FIGURE 3: (a) Initially spherical grains before deformation and (b) elongated grains due to deformation.

shown in Figure 3(a). As the materials were subjected to deformation it was observed that the semimajor axis radius r_1 and major axis radius r_3 initially increased (as shown in Figure 3(b)) and then decreased since grain breakages took place in these directions. As a result of this repeated lengthening and grain breakage processes the effective lengths of r_1 and r_3 decreased during grain refinement. It was also observed during grain refinement that the equivalent radius axis r and semiminor axis radius r_2 decrease continuously. It was further observed that r_2 and r_3 evolved as proportions or fractions of r and r_1, respectively.

2.6. Models Derivation. The model for grain elongation in *2D* [12] can be modified to be applicable to *3D* grain from the previous work of Sob et al. [13] for grain elongation in 2D to grain elongation in 3D grain by relating the cross-sectional area A of a *2D* grain given in the previous model [12] from [13] to the volume in *3D* grain of [13] since in *3D* the density of a material is determined by it volume. This relationship is given as $A = V^{2/3}$. Thus the expression of elongation as defined by Nash [12] is modified to

$$\text{Elongation} = \frac{Pr_0}{V^{2/3}E}, \tag{1}$$

where r_0 is initial length, E is Young's modulus, and P is the applied force.

The model for Young's modulus (E) of nanomaterials as defined by Sob et al. [14] is given as

$$E = \left(\frac{P}{d}\right)\left(\frac{r^3}{192I}\right), \tag{2}$$

where it can be inferred that the moment of inertial is $I = \pi r_1^4/64$, $d = dr = (r - r_0)$, and r is length or equivalent radius of nanocrystalline grain.

It is experimentally observed during grain size evolution that at any instant the radii can be related to the equivalent volume of the grain through $(4/3)\pi r^3 = V = (4/3)\pi r_1 r_2 r_3$. This gives

$$r^3 = r_1 r_2 r_3. \tag{3}$$

By substituting expressions (2) and (3) into expression (1), the derived model of elongation for *3D* grain is given as

$$\text{Elongation} = \frac{3\pi r_0 r_1^4}{r_2 r_3 r^3}\left(r - r_0\right). \tag{4}$$

By employing the different experimental observations for r, r_1, r_2, and r_3 during grain refinement, the following set of grain size variant evolutions (given in expressions (5)–(8)) were established for *3D* grain as defined by Sob et al. [14] as follows.

Since r_1 increased and instantaneously decreased after breakage, the evolution of r_1 during grain refinement can be represented as

$$dr_1 = M\left(\frac{1}{r_{c1}} - \frac{1}{r_1}\right)dt + r_1^{1/2}DdW(t) - Zr_1V_1d(t), \tag{5}$$

where r_{c1} is local critical grain size, Z and D are constants, $dW(t)$ is change of the Wiener process, $V_1 = \tau_1 r_1^2$ defines rate of grain breakage, $M = M_o(1 + CD/r_1)$, $CD = 4(Hm)(h_o)/((k)(T))$, $T_m = T\{\ln(M_{o1}/M)\}$, and $M_O = M_{O1}\exp\{(\inf)/T\}$ as given by [6, 10].

Since r_3 evolves (i.e., decreases) as a fraction or proportion (Ratio_1) of r_1 during grain refinement, r_3 can be represented by

$$dr_3 = \text{Ratio}_1\left(dr_1\right). \tag{6}$$

Since equivalent radius r decreases continuously during grain refinement, r can be represented by

$$dr = -Ordt + IdW(t), \tag{7}$$

where O and I are constants.

For r_2 that evolves or decreases as a fraction (Ratio_2) of r during grain refinement, r_2 can be represented by

$$dr_2 = \text{Ratio}_2\left(dr\right). \tag{8}$$

Moving now to other mechanical properties, the model of the yield stress given by Reversed Hall-Petch Relationship (RHPR) as modified by Zhao and Jiang [9] is given by

$$\sigma(r) = \sigma_0' + A\left(r^{-1/2}\right) - B\left(r^{-1}\right) - C\left(r^{-3/2}\right), \tag{9}$$

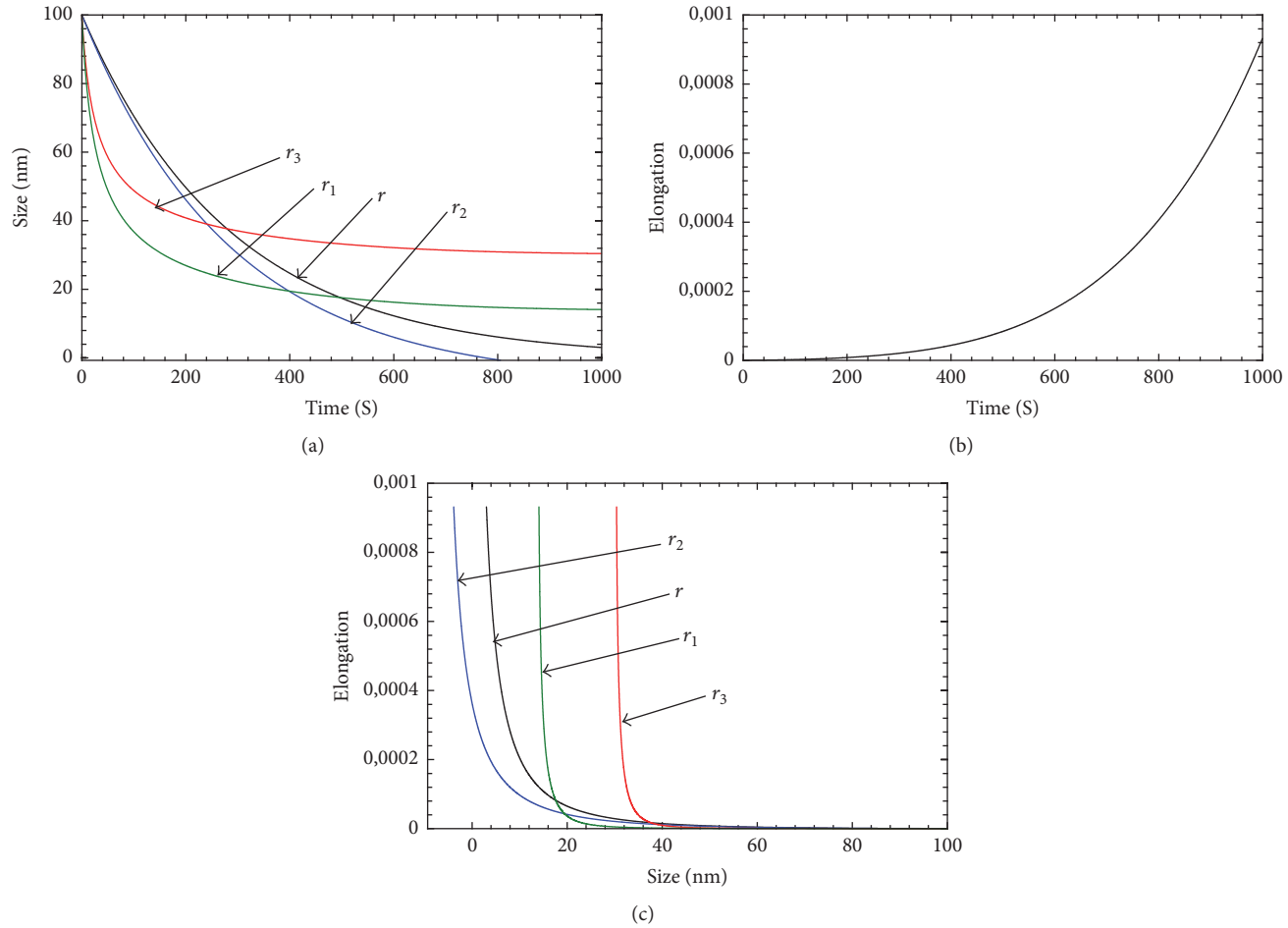

FIGURE 4: (a) Time evolution of size, (b) time evolution of elongation, and (c) evolution of elongation as function of size.

where $\sigma_0' = \sigma_0 + K_t$ is bulk yield stress, $A = K_d$ is HPR proportionality constant, $B = K_t[2hH_m/RT_r]$, $C = K_d[2hH_m/RT_r]$, K_t is a constant, h is atomic diameter in the case of metal, H_m is the bulk melting enthalpy, R is ideal gas constant, and T_r is the room temperature, $K_d \rangle 100K_t$ and $\sigma_0 \rangle 10K_t$.

The models of strain evolution for nanocrystalline material for the different approaches of measuring grain size evolution given in expressions (5)–(8) as defined by Sob et al. [14] are as follows:

$$d\varepsilon_1 = d\left[\frac{dr_1}{r_1}\right] = d\left(M\left(\frac{1}{r_{1c}}\right)\left(\frac{1}{r_1}\right) - \frac{1}{r_1^2}\right)dt + \frac{CDdW(t)}{r_1} - \frac{ZV_1 r_1^2 d(t)}{r_1},$$

$$d\varepsilon_3 = d\left[\frac{dr_3}{r_3}\right] = d\left(\frac{\text{Ratio}_1 dr_1}{r_3}\right),$$

$$d\varepsilon_r = d\left[\frac{dr}{r}\right] = d\left(\frac{-Ordt + IdW(t)}{r}\right),$$

$$d\varepsilon_2 = d\left[\frac{dr_2}{r_2}\right] = d\left(\frac{\text{Ratio}_2 dr}{r_2}\right). \quad (10)$$

Equations (1) to (10) are solved simultaneously using Engineering Equation Solver software (F-Chart Software, Madison, W153744, USA) while employing the lognormal distribution of grain size.

3. Results and Discussion

To test the models proposed in this paper, the data from (nanocrystalline) aluminum sample (some of which are found in other papers [6]) are used, which are $M_0' = 0.01\,\text{nm}^2\text{s}^{-1}$, $m = 4$, $CC = 12$, $a = 0.90$, $D = 10^{-4}$, $h_0 = 0.25\,\text{nm}$, $T_m(\infty) = 933.47\,\text{K}$, $CV_0 = 0.3$, $H_m(\infty) = 10.71\,\text{KJMol}^1$, $\sigma_0' = 16.7\,\text{MPa}$, $K_t = 1.3$, $\sigma_0 = 15.40\,\text{MPa}$, $K_d = 1301.77\,\text{MPa\_nm}^{1/2}$, $R = 8.31\,\text{JK}^{-1}\,\text{mol}^{-1}$, and $T_r = 300\,\text{K}$. The additional data obtained for this work are $O = 0.0035$, $I = 1.1$, $r_{c1} = 1.95r$, $r_0 = 100\,\text{nm}$, $Z = 0.4$, $\text{Ratio}_1 = 0.81$, $\text{Ratio}_2 = 1.071$, and $\tau_1 = 0.000008$. The obtained results are presented in Figures 4(a), 4(b), and 4(c).

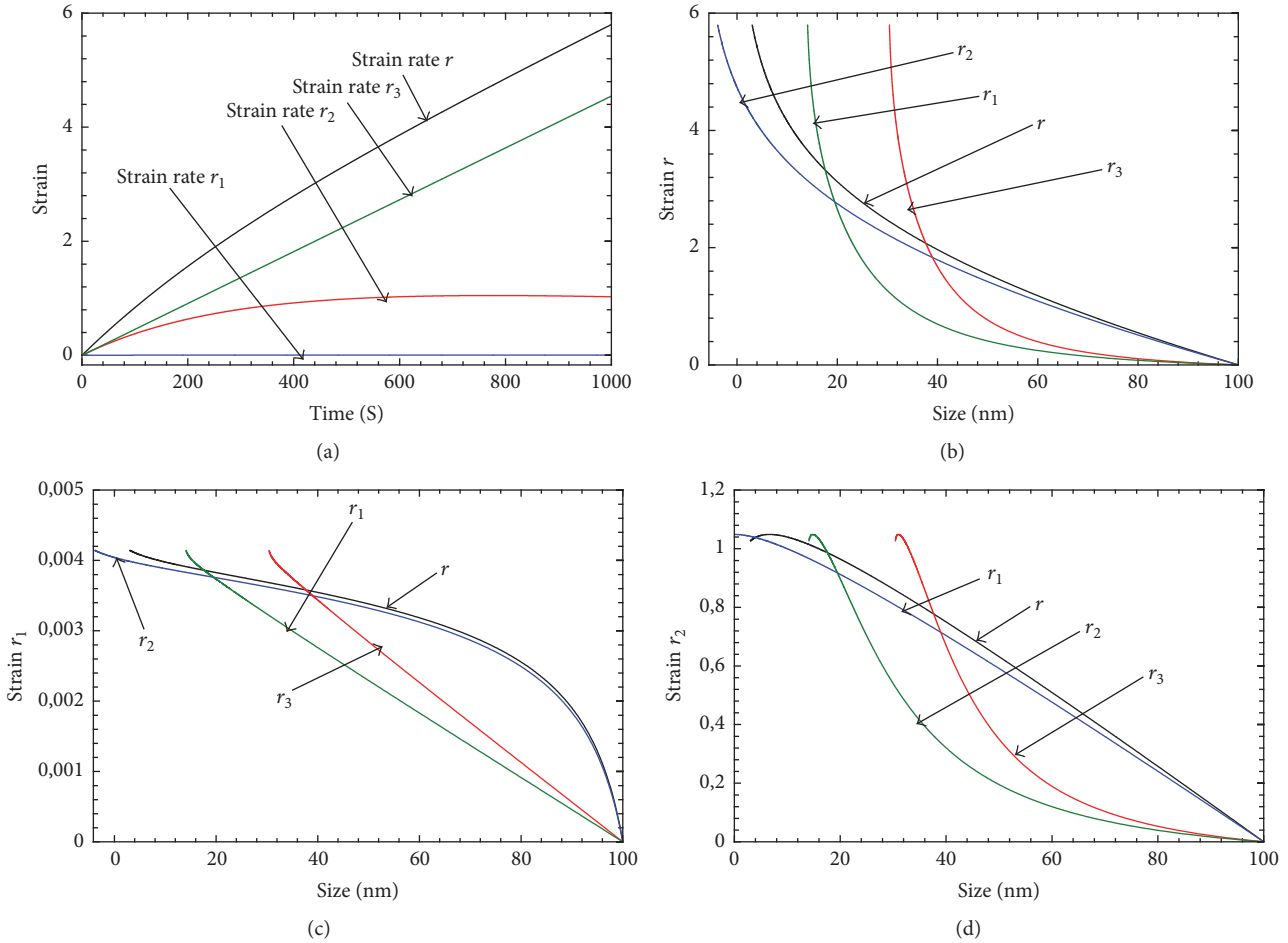

Figure 5: (a) Time evolutions of strains and ((b)–(d)) strain evolutions as functions of grain size variants (nm).

It should be observed from Figure 4(a) that the natures of decrease of the different approaches of measuring grain sizes are typical of experimental revelations of *3D* grains. The different approaches of measuring grain size such as r_1, r_2, r_3, and r have different characteristics and hence different properties (yield stress) due to different grain orientation and grain curvatures as shown in Figures 3(a) and 3(b). Since grain breakage rotation, grain migration, and grain rotation coalescence events take place during grain refinement by ARB and ECAP whose rates depend on grain curvature or elongation, different material yield stresses are being reported as shown in Figures 3(a) and 3(b). It should be observed from Figure 4(a) that r_2 decrease as lower value when compared to r throughout the deformation process, and, similarly, r_1 decrease as lower value when compared with r_3 throughout the deformation range. It was also observed that both r_1 and r_3 initially started with breakage and as such smaller grain sizes, which then lengthened and became larger than the sizes of r and r_2. The increase in grain elongation with time as shown in Figure 4(b) or with decreasing grain size as shown in Figure 4(c) can be explained by the fact that, during grain refinement, new high angle grain boundaries are generated. It is noted further from Figure 4(c) that, depending on the approach of measuring grain size or observing the grain size, the elongation values can become so *large at larger grain size* or the elongation values become *larger at smaller* grain size.

It is shown from Figure 5(a) that, at a time of, for example, 600 sec, different strains are obtained for the different approaches of measuring grain size. The nature of the evolution of strains depends on the direction along which the grain size is measured, as shown in Figures 5(b)–5(d). The reasons for this nature of evolution of strain values with respect to the different directions of observation (of the grain size) are that it was noted experimentally that, along the axial (r_1) and lateral (r_3) directions, both change-in-grain size and grain size varied proportionately with both either increasing or decreasing simultaneously, while, along the normal direction (r_2) or equivalent radius measured (r), the increasing change-in-grain sizes were accompanied by reductions in the grain sizes making the strains approach infinite values.

From Figure 6 it is observed that yield stress evolved as predicted by Hall-Petch to Reversed Hall-Petch Relationship (HPR-RHPR) when measured as functions of time, different approaches of measuring grain size, elongation, strain, and strain rate. The yield stress generally tended to increase with decreasing gain size since it is reported [14, 15] to be a result of dislocation motion from grain interiors to grain

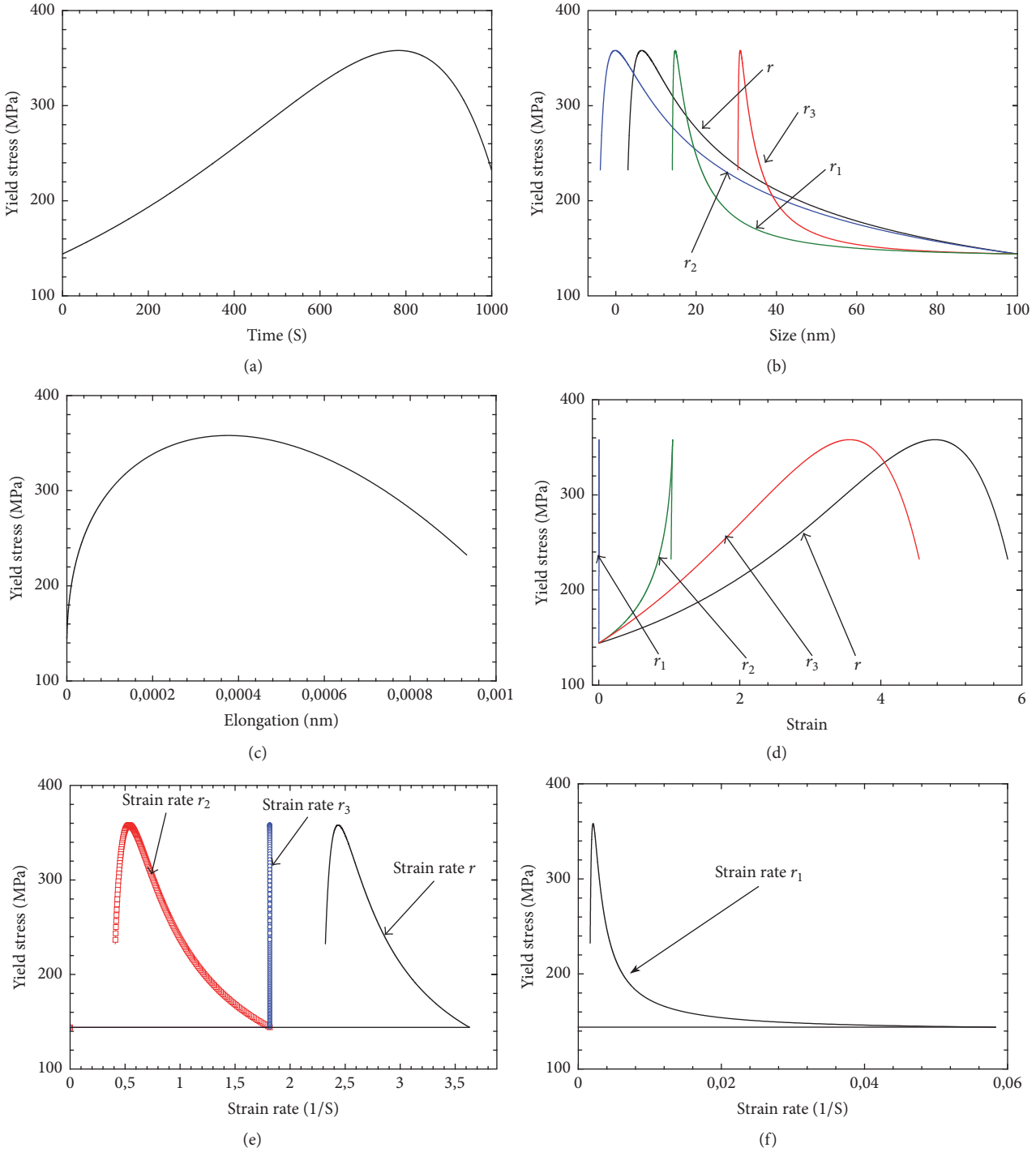

FIGURE 6: Plots of yield stress as a function of (a) time, (b) size, (c) elongation, (d) strain, and ((e)-(f)) strain rate.

boundaries and subsequent dislocation pile-ups at the grain boundaries. It was observed that, in the directions whereby the sizes increased and subsequently decreased due to grain breakage (i.e., r_1 and r_3), there were more material flow in those directions, which can without loss of generality be claimed that there were more dislocation motions and pile-ups towards those directions and hence more grain boundary curvatures in those directions. As a result the yield stress when measured as a function of grain size and strain with size measured along the r_1 and r_3 directions show more rapid enhanced properties (see Figures 6(b) and 6(d)). Since elongation can be termed lengthening, it can be concluded that materials with elongated grains have more enhanced properties which rapidly drop with continuous lengthening

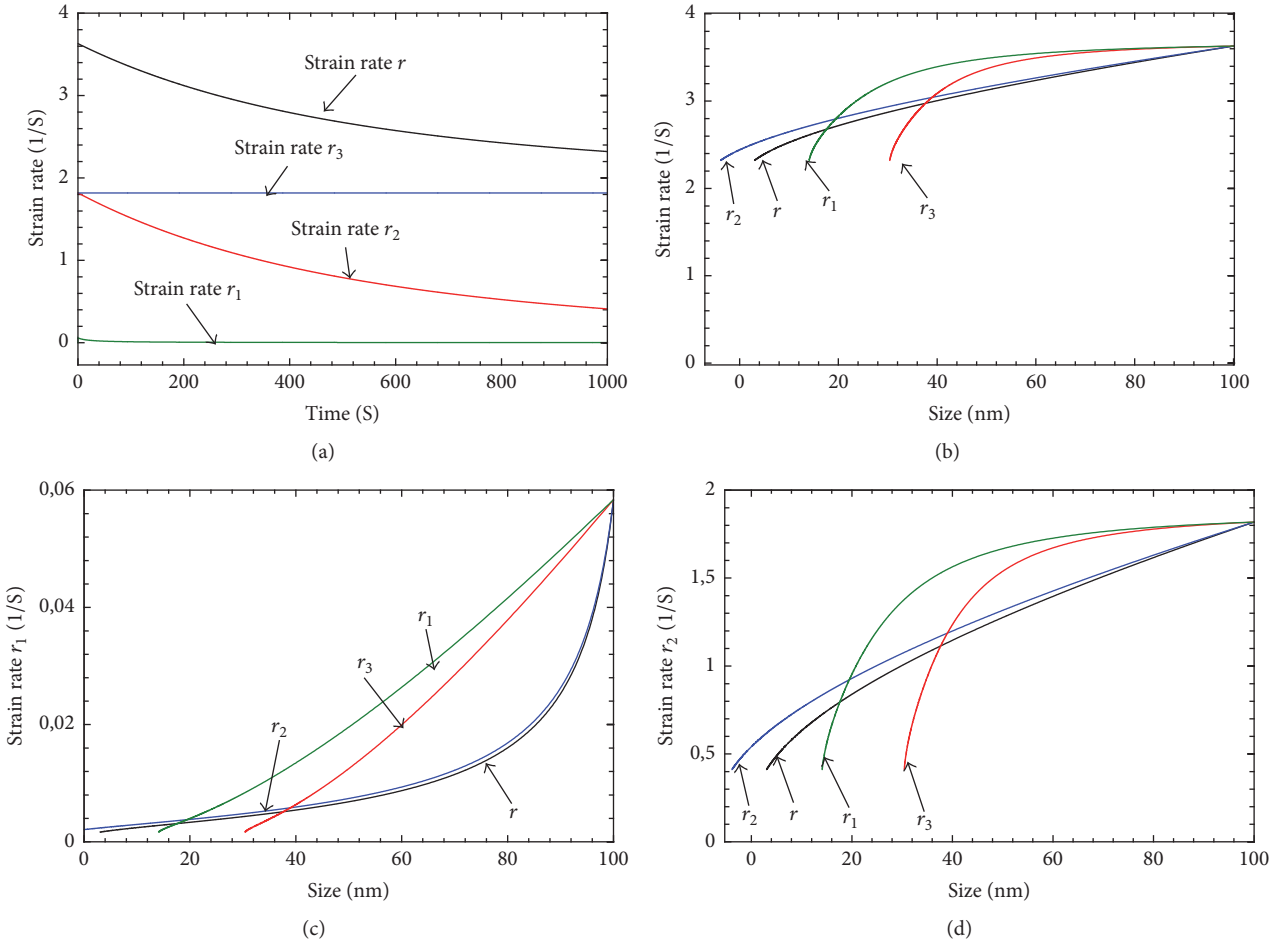

Figure 7: Plots of strain rate as a function of (a) time and (b)–(d) size (nm).

of grains, as revealed in Figures 6(b), 6(c), and 6(d) and for most ARB processes at rolling facilities. The reason for the subsequent decrease in yield stress with further decrease in grain size was that low plastic deformation occurred resulting in low materials hardness and properties. Extreme plastic straining led to distorted structures where the grain boundaries and grain curvatures were in "nonequilibrium" states. At these nonequilibrium states the grain boundaries and grain curvatures are characterized by more grain boundary energy, enhanced free volume, and the presence of long range elastic stresses [16].

Studying the effect of curvature on properties, reference is made to Figure 6(b). From the figure it is noted that, at grain size of 35 nm, the material has the most enhanced property (i.e., yield stress) for radius measured along r since the grain curvature of Cr is higher than the grain curvature of $Cr1$, $Cr2$, and $Cr3$ at that 35 nm. When the material gets more refined at a size of 30 nm, the material has the most enhanced property for the radius measured along r_3 since grain curvature for $Cr3$ is higher than the grain curvature of $Cr1$, $Cr2$, and Cr. Furthermore, it has been revealed as shown in Figure 6(b) that different critical grain sizes exist for r_1, r_2, r_3, and r but give the same yield stress value at those different critical grain sizes. It is observed from Figure 6(d) that the yield stresses for the grain size variants increase with increasing strains due to different misorientation angles and the grain curvatures ($Cr1$, $Cr2$, $Cr3$, and Cr) during grain deformation.

The different strain rates observed in Figures 6(e) and 6(f) have a general trend. This implied that in order to increase the material yield stress the rate of straining the material had to be reduced, similar to observations made by other researchers [16–18]. This is required so as to allow the material to relax and accommodate more plastic strain. Furthermore, it is observed that indefinite reduction in strain rate or feed rate does not lead to more property enhancement since it was becoming difficult for the material to be gripped by the rollers and get deformed. It was also noted that the rate of straining the material depended on the direction of observation or measuring the grain size. Figure 7 shows that in order to have more grain refinements the strain rates have to be decreased.

4. Conclusions

The current work was aimed at investigating the impacts of elongation or grain shapes on nanomaterials properties. To achieve that, the model for elongation that has been

previously given for *2D* was modified to be applicable to *3D* grains. Furthermore, the stochastic natures of the grain size variants (i.e., different approaches of measuring or observing grain sizes) were also taken into consideration.

It was observed that the stochastic effect of grain elongation led to different mechanical properties when studied as functions of different grain size variants due to different grain curvatures. It was shown that the properties varied in different ways with equivalent radius, semiminor axis radius, semimajor axis radius, and major axis radius. The present analysis revealed that the material has the most enhanced property for radius measured with higher grain curvature and less enhanced property for radius with low grain curvature. It has also been revealed that in order to increase the material yield stress the rate of straining the material has to be reduced. It was also observed that materials with elongated grains have more enhanced properties that rapidly drop with continuous lengthening of grains. The present analysis for *3D* grain shows more properties for nanomaterials that were not revealed from the models that dealt only with the equivalent radius. These findings provide valuable insights into the possibility of tailoring sample dimensions to elicit desired property.

Disclosure

The abstract of this manuscript was approved at the international conference of composites materials held in Istanbul 2015 but the full paper was not submitted for journal consideration at the conference.

Conflicts of Interest

The authors declare that they have no conflicts of interest.

Acknowledgments

This paper is based on the work which is supported financially by the National Research Foundation (NRF) and Vaal University of Technology (VUT).

References

[1] Y. Estrin and A. Vinogradov, "Extreme grain refinement by severe plastic deformation: a wealth of challenging science," *Acta Materialia*, vol. 61, no. 3, pp. 782–817, 2013.

[2] M. Saravanan, R. M. Pillai, B. C. Pai, M. Brahmakumar, and K. R. Ravi, "Equal channel angular pressing of pure aluminium-an analysis," *Bulletin of Materials Science*, vol. 29, no. 7, pp. 679–684, 2006.

[3] N. Tsuji, Y. Saito, S.-H. Lee, and Y. Minamino, "ARB (accumulative roll-bonding) and other new techniques to produce bulk ultrafine grained materials," *Advanced Engineering Materials*, vol. 5, no. 5, pp. 338–344, 2003.

[4] A. Rosochowski, L. Olejnik, J. Richert, M. Rosochowska, and M. Richert, "Equal channel angular pressing with converging billets-experiment," *Materials Science and Engineering A*, vol. 560, pp. 358–364, 2013.

[5] M. Hillert, "On the theory of normal and abnormal grain growth," *Acta Metallurgica*, vol. 13, no. 3, pp. 227–238, 1965.

[6] T. B. Tengen, *Analysis of Characteristic of Random Microstructures of Nanomaterials [PhD. Thesis]*, Witwatersrand Johannesburg, 2008.

[7] E. O. Hall, "The deformation and ageing of mild steel: III discussion of results," *Proceedings of the Physical Society Section B*, vol. 64, no. 9, pp. 747–753, 1951.

[8] N. J. Petch, "The cleavage strength of polycrystasl," *Journal of the Iron and Steel Institute*, vol. 174, pp. 25–28, 1953.

[9] M. Zhao and Q. Jiang, "Reverse hall-petch relationship of metals in nanometer size," in *Proceedings of the 2006 IEEE Conference on Emerging Technologies—Nanoelectronics*, pp. 472–474, Singapore, January 2006.

[10] T. B. Tengen, T. Wejrzanowski, R. Iwankiewicz, and K. J. Kurzydlowski, "Stochastic modelling in design of mechanical properties of nanometals," *Materials Science and Engineering A*, vol. 527, no. 16-17, pp. 3764–3768, 2010.

[11] M. Lewandowska, "Malgorzata lewandowska: fabrication methods of nanomaterials," in *Structure and Properties of Nanomaterials*, pp. 1–54, 2006.

[12] W. A. Nash, *Strength of Materials*, McGraw-Hill, New York, NY, USA, 4th edition, 1998.

[13] P. B. Sob, A. A. Alugongo, and T. B. TengeN, "Stochastic effect of grain elongation on nanocrystalline material yield stress produced by accumulative roll bonding," in *Proceeding of the 9th South African Conference of Computational and Applied Mechanics (SACAM '14)*, Somerset West, South Africa, 2014.

[14] P. B. Sob, A. A. Alugongo, and T. B. Tengen, *Modelling Strain Rate Sensitive Nanomaterials Mechanical Properties: The Effects of Varying Definition. MTECH, [MS thesis]*, Vaal University of Technology, Vanderbijlpark, South Africa, 2016.

[15] G. Wang and L. Xiaodong, "Predicting the young's modulus of nanowire from first principle calculations on their surface and bulk materials," *Journal of Applied Physics*, vol. 104, no. 11, Article ID 113517, pp. 1–33, 2008.

[16] K. M. Rahman, V. A. Vorontsov, and D. Dye, "The effect of grain size on the twin initiation stress in a TWIP steel," *Acta Materialia*, vol. 89, pp. 247–257, 2015.

[17] L. S. Toth and C. Gu, "Ultrafine-grain metals by severe plastic deformation," *Materials Characterization*, vol. 92, pp. 1–14, 2014.

[18] I. Sabirov, M. R. Barnett, Y. Estrin, and P. D. Hodgson, "The effect of strain rate on the deformation mechanisms and the strain rate sensitivity of an ultra-fine-grained Al alloy," *Scripta Materialia*, vol. 61, no. 2, pp. 181–184, 2009.